International Journal of Electrical and Computer Engineering (IJECE)
Vol. 7, No. 3, June 2017, pp. 1188~1196
ISSN: 2088-8708, DOI: 10.11591/ijece.v7i3.pp1188-1196

Novel Image Mosaicking of UAV's Imagery using Collinearity Condition

Martinus Edwin Tjahjadi[1], Fourry Handoko[2], Silvester Sari Sai[3]
[1,3]Departement of Geodesy, National Institute of Technology (ITN) Malang, Indonesia
[2]Departement of Industrial Engineering, National Institute of Technology (ITN) Malang, Indonesia

Article Info

Article history:

Received Jan 12, 2017
Revised May 18, 2017
Accepted May 30, 2017

Keyword:

Collinearity condition
Computer algorithm
Image mosaicking
Image processing
UAV

ABSTRACT

This paper presents a preliminary result of ongoing research on unmanned aerial vehicle (UAV) for cooperative mapping to support a large-scale urban city mapping, in Malang, Indonesia. A small UAV can carry an embedded camera which can continuously take pictures of landscapes. A convenient way of monitoring landscape changes might be through accessing a sequence of images. However, since the camera's field of view is always smaller than human eye's field of view, the need to combine aerial pictures into a single mosaic is eminent. Through mosaics, a more complete view of the scene can be accessed and analyzed. A semi-automated generation of mosaics is investigated using a photogrammetric approach, namely a perspective projection which is based on collinearity condition. This paper reviews the general projection model based on collinearity condition and uses that to determine a common projective plane from images. The overlapped points for each RGB channel are interpolated onto that of orthographic plane to generate mosaics. An initial attempt shows a promising result.

Corresponding Author:

Martinus Edwin Tjahjadi,
Departement of Geodesy,
National Institute of Technology (ITN) Malang,
Jl. Bendungan Sigura-gura No.2 Malang 65145, Jawa Timur, Indonesia.
Email: edwin@lecturer.itn.ac.id

1. INTRODUCTION

Mosaic is a single continuous composite image formed by piecing together two or more overlapping aerial images [1]. It is not a truly representation of a planimetric map since perspective images are being used to construct it. Although it is subject to relief displacements and scale variations due to variation in the terrain elevations and tilting of the camera axis, it gains popularity for qualitative and interpretative studies. It can be categorized into three types of a mosaic [1], namely controlled, semi-controlled, and uncontrolled mosaic. A controlled mosaic is created from individually rectified and equally scaled images. A set of surveyed ground control points (GCPs) are provided to constrain the position of images. Image positions of conjugate and repeatable common features as well as the GCP features on adjacent images are matched and pieced them together to form the mosaic. On the other hand, an uncontrolled mosaic is assembled by simply matching conjugate features of adjacent images, and there are no GCPs or rectification and scaling of images involved. This is the least accurate of mosaic types. A semi-controlled mosaic is assembled by using a combination of the specifications for the controlled and uncontrolled mosaic. For example, this mosaic is prepared by using GCPs but employing unrectified and unscaled images. The other combination would be to utilize rectified and scaled images but no GCPs.

There are many mosaic techniques available [2], [3]. Basically a four general steps for assembling a mosaic are identified whatever technique is selected, namely feature extraction, image registration, homography finding, and image warping and blending [4-6]. Main approaches of performing image

regristration utilize feature-based methods [2], [7], while homography finding is performed using RANSAC algorithm [3]. For photogrammetric and mapping related purposes, these methods are less suitable for producing qualitative mosaics since influences of perspectivities are still occur such as uneven scales.

To alleviate this problem, this paper focuses on a novel image registration and homography techniques by modifying a collinearity condition to transform images into a mosaic using perspective projection of image planes. Specifically, the steps to build a mosaic are discussed as follows: determine point correspondences between images, estimate transformation parameters between pairs of images, and compute the extent of the output mosaic. Furthermore, this paper discusses a possibility to assembly the uncontrolled mosaic by using equally scaled images through projecting images into an arbitrary planar surface. A simplified collinearity condition of planar surface is derived to a common projective plane from images.

2. RESEARCH METHOD

In this research, a fixed-wing UAV based spatial information acquisition platform which can carry a digital camera on board is developed. Such a system provides only a navigation-grade of the position and orientation of exposure stations. This system only has a C/A code GPS and a low cost Inertial Measurement Unit (IMU), Micro Electro-Mechanical systems (MEMS), and they can be immediately embedded into UAV to facilitate an autonomous flight [8]. This navigation solution (position and attitude) is estimated by the internal UAV sensor and usually can be used to directly georeference the images to produce a quick and easy description of the area. As a result it is very rarely to obtain true vertical images as it is prerequisite for photogrammetric mosaicking. Based on the navigation solution, it can be calculated a mathematically horizontal plane above a datum that acts like a canvas for compositing images into a mosaic, as illustrated in Figure 1.

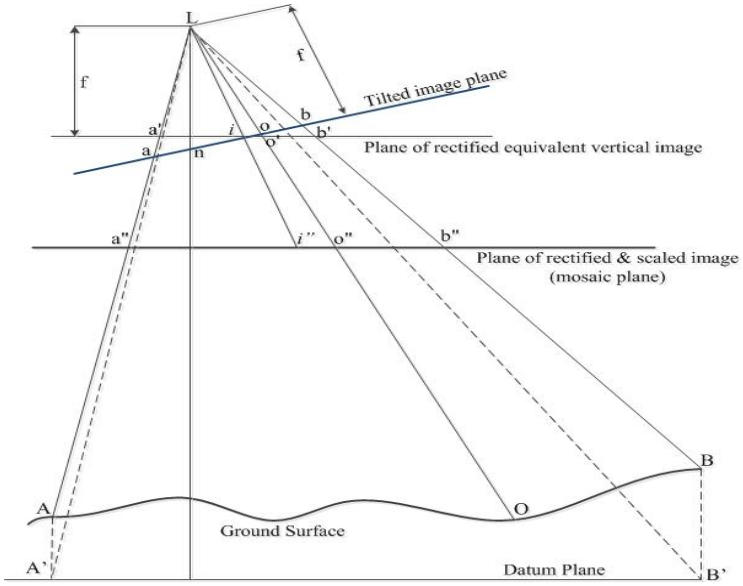

Figure 1. A basic geometry of assembling tilted images into a mosaic.

Figure 1 explains the fundamental geometry of image mosaicking and it shows a side view of the tilted image plane when the exposure was made. Rays from A and B were imaged at point a and b on the tilted image. The plane of equivalent vertical image is shown parallel to the datum plane and passing through i, the isocenter of the tilted image. The plane of the mosaic is likewise parallel to the datum plane but exists at a level other than that of the rectified and scaled image plane. In assembling the controlled mosaic, tilted images must undergo a rectification to become equivalent vertical images and they are stitched together on the mosaic plane at an equal scale. However, the rectification process is not necessary for assembling the uncontrolled mosaic [9].

In this paper, the algorithm for the uncontrolled mosaic starts with an image selection which has a minimum angle of tilt and it was rectified by using an open source tool. By setting this image as a mosaic plane, all the remaining images are stitched onto that image. The image mosaicking system utilizes a combination of manual user input for registration between images. Using our own developed software, a user

can select a feature by clicking over it and its corresponding points from other overlapped image are automatically selected within sub-pixel accuracy. This process is repeated for all images until the number of minimum conjugate points of four is reached. This sub-pixel matcher enables the image matching algorithm find matched points accurately.

2.1. Point Correspondences using Area based Image Matching

The term 'image matching' refers to the process of finding corresponding or conjugate points in digital images (or parts thereof) in the form of a matrix of reflectance levels [10]. Area based matching is based on the idea that grey values of pixels of conjugate points have similar radiometric characteristics [11]. The process generally requires a close approximation to the matched patches in order to ensure a successful match. In other words, having a point in one image, its conjugate in the other one is obtained by optimizing a certain similarity measure, defined over the pixel grey values within the image window. Two techniques are adopted to calculate the possible similarity measures within sub-pixel accuracy: a normalized correlation coefficient method [7], [12, [13] and a least square matching method[10], [14].

$$\rho = \frac{\sum_{i=1}^{m}\sum_{j=1}^{n}\left[\left(f_{ij}-\bar{f}\right)\left(g_{ij}-\bar{g}\right)\right]}{\sqrt{\left[\sum_{i=1}^{m}\sum_{j=1}^{n}\left(f_{ij}-\bar{f}\right)^{2}\right]\left[\sum_{i=1}^{m}\sum_{j=1}^{n}\left(g_{ij}-\bar{g}\right)^{2}\right]}} \quad (1)$$

Equation (1) is a normalized cross correlation method, where ρ is the normalized cross-correlation coefficient; m and n are the numbers of rows and columns of the patches respectively; f_{ij} is the i^{th} row and j^{th} column of the grey value from the template patch; g_{ij} is the i^{th} row and j^{th} column of the grey value from the target patch; $\bar{f}$ and $\bar{g}$ are the arithmetic means of the grey values in the template patch and the target patch, respectively (Figure 2).

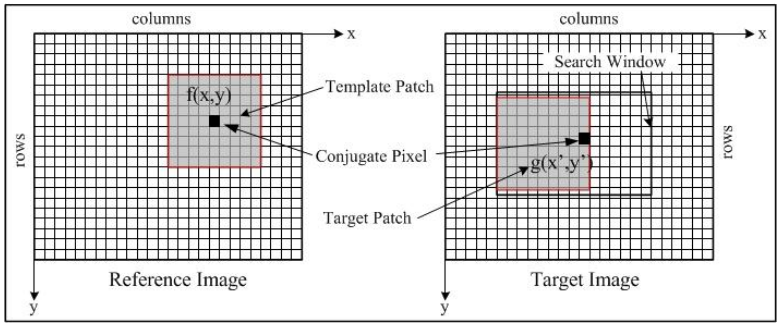

Figure 2. The concept of area based matching

The correlation coefficient can range from -1 to +1 with +1 indicating an exact match. A coefficient of -1 indicates negative correlation which would occur if images from a photographic negative and positive were being compared, whereas coefficient values near zero indicate a non-match. Due to factors such as image noise, perfect (+1) correlation is a rare case. Generally, to identify pattern positions in the search window, all x, y positions with correlation coefficients greater than a threshold value are assumed to indicate a valid match of the patches. The choice of a suitable threshold value depends on the image content, and a suitable threshold value for stereo images lies in the range between 0.5 and 0.7 [1]. Despite its computational simplicity, it is computationally expensive considering that correlation coefficient is calculated at every pixel in two directions over a given patch in the search window. Another major disadvantage of this method is that it neither takes into account the fact that there may be geometric and radiometric differences between the two patches being matched, nor adapts to distortions caused by scale and perspective differences between images, different lighting condition, and high frequency noise contaminations. Consequently, the match determined by this technique is error prone, and can often produce a misleading match.

To seek a better match, a Least Square Matching (LSM) technique is utilized. This method employs iterative radiometric and geometric transformations between the template patch f(x, y) of n x n pixels and the

target patch g(x, y) of an equal size. The objective of LSM is to estimate a new location of g(x, y) such that the grey value differences between f(x, y) and g(x, y) are minimized [14]:

$$f(x, y) = g(x, y) + e(x, y) \quad (2)$$

e(x, y) is the true error vector of a goal function, which measures the differences of grey values between the template patch and the target patch. A linearization of the Equation (2) gives:

$$f(x, y) = g^{\circ}(x, y) + \frac{\partial g^{\circ}(x,y)}{\partial x} dx + \frac{\partial g^{\circ}(x,y)}{\partial y} dy + e(x, y); \; dx = \frac{\partial x}{\partial p_i} dp_i; dy = \frac{\partial y}{\partial p_i} dp_i \quad (3)$$

p_i are the geometric transformation parameters. An appropriate numbers of parameters p must be considered to avoid problems of over-parameterization. Because image patches are usually very small, a further simplification can be introduced via affine transformation, which is considered to be a sufficiently full parameter set. In the case of affine transformation, the transformed matching patch is obtained from the original as follows [10]:

$$x = a_1 + a_2 x_0 + a_3 y_0 \;\; ; \;\; y = b_1 + b_2 x_0 + b_3 y_0 \quad (4)$$

where x_o and y_o are the coordinates of the data points $g^{\circ}(x, y)$; a_1 and b_1 represent the shift parameters of Δx and Δy respectively; and a_2, a_3, b_2, and b_3 are the shaping parameters. Differentiation provides:

$$dx = da_1 + x_o \, da_2 + y_o \, da_3 \;\; ; \;\; dy = db_1 + x_o \, db_2 + y_o \, db_3 \quad (5)$$

Equation (2) is then modified to become:

$$f(x, y) = g^{\circ}(x, y) + g_x \, dx + g_y \, dy + e(x, y); \;\; g_x = \frac{\partial g^{\circ}(x,y)}{\partial x}; \;\; g_y = \frac{\partial g^{\circ}(x,y)}{\partial y} \quad (6)$$

The g_x and g_y in Equation (6) are a discrete first derivative (or a gradient) in the x-direction and in the y-direction, respectively. Derivatives of images can be approximated by the following central-difference approximations [15]:

$$\begin{aligned} g_x &= \frac{I(i+1,j) - I(i-1,j)}{2} \;\; ; \;\; \text{or} \;\; g_x = \frac{-I(1+2,j) + 8I(i+1,j) - 8I(i-1,j) + I(i-2,j)}{12} \\ g_y &= \frac{I(i,j+1) - I(i,j-1)}{2} \;\; ; \;\; \text{or} \;\; g_y = \frac{-I(i,j+2) + 8I(i,j+1) - 8I(i,j-1) + I(i,j-2)}{12} \end{aligned} \quad (7)$$

The grey values of f(x, y) and g(x, y) are generally going to differ due to other factors such as temporal differences of illumination source radiance, different distance and viewing angles of the cameras to the object, lens distortion, and errors in image acquisition. To compensate for these errors and acquire a better match, a set of radiometric transformation parameters for g(x, y) is incorporated. Two radiometric parameters, r_o (grey value shift) and r_1 (grey value scale), are introduced into the system of (6) and it gives a result as follows:

$$f(x, y) = g^{\circ}(x, y) + g_x \, dx + g_y \, dy + e(x, y) + r_o + r_1 \, g^{\circ}(x,y) \quad (8)$$

If Equation (5) is substituted to Equation (9), it gives the result:

$$\begin{aligned} f(x, y) = {} & g^{\circ}(x, y) + e(x, y) + g_x \, da_1 + g_x \, da_2 + g_x \, da_3 \\ & + g_y \, db_1 + g_y \, db_2 + g_y \, db_3 + r_o + r_1 \, g^{\circ}(x,y) \end{aligned} \quad (9)$$

Then Equation (9) can be solved by Gaussian Least Square Adjustment to give the conjugate points between images and mosaic.

2.2. Perspective Transformation

In Figure 1, it shows that rays from A and B on the ground surface which piercing the mosaic plane at a" and b" and the image plane at a and b are passing to the perspective center L as a straight line. This situation can be expressed mathematically as a collinearity condition between a point on the ground and camera system [1]:

$$\begin{aligned} x &= x_o - f\frac{m_{11}(X-X_o)+m_{12}(Y-Y_o)+m_{13}(Z-Z_o)}{m_{31}(X-X_o)+m_{32}(Y-Y_o)+m_{33}(Z-Z_o)} \\ y &= y_o - f\frac{m_{21}(X-X_o)+m_{22}(Y-Y_o)+m_{23}(Z-Z_o)}{m_{31}(X-X_o)+m_{32}(Y-Y_o)+m_{33}(Z-Z_o)} \end{aligned} \quad (10)$$

where (x, y) and (X, Y, Z) are photo coordinates and mosaic coordinates respectively, (x_o, y_o, f) are interior orientation parameters, (m_{11}, …, m_{33}) are rotation matrix coefficients, and (Z_o, Y_o, Z_o) are exposure camera coordinates. Since the mosaic plane has equal elevations, a coordinate system in the object plane with Z = 0 should be preferred. The collinearity condition of Equation (10) is reduced to:

$$\begin{aligned} x &= x_o - f\frac{m_{11}(X-X_o)+m_{12}(Y-Y_o)+m_{12}(-Z_o)}{m_{31}(X-X_o)+m_{32}(Y-Y_o)+m_{33}(-Z_o)} \\ y &= y_o - f\frac{m_{21}(X-X_o)+m_{22}(Y-Y_o)+m_{23}(-Z_o)}{m_{31}(X-X_o)+m_{32}(Y-Y_o)+m_{33}(-Z_o)} \end{aligned} \quad (11)$$

Equation (11) contains a total of nine parameters $(x_o, y_o, f, \omega, \phi, \kappa, X_o, Y_o, Z_o)$ as well as the measured coordinates x, y, X and Y in two coordinate systems. A further simplification of Equation 12 can reduce the number of parameters to 8 only [16] which is common for the image to mosaic transformation process:

$$x = \frac{a_1X + b_1Y + c_1}{a_3X + b_3Y + 1} \;;\; y = \frac{a_2X + b_2Y + c_2}{a_3X + b_3Y + 1} \quad (12)$$

where:

$$\begin{aligned} a_1 &= (m_{31}x_o - m_{11}c)/G \quad ; \quad a_2 = (m_{31}y_o - m_{21}c)/G \\ b_1 &= (m_{32}x_o - m_{12}c)/G \quad ; \quad b2 = (m_{32}y_o - m_{22}c)/G \\ c_1 &= x_o + c(m_{11}X_o + m_{12}Y_o + m_{13}Z_o)/G \quad ; \quad a_3 = m_{31}/G \\ c_2 &= y_o + c(m_{21}X_o + m_{22}Y_o + m_{23}Z_o)/G \quad ; \quad b_3 = m_{32}/G \\ G &= -(m_{31}X_o + m_{32}Y_o + m_{33}Z_o) \end{aligned} \quad (13)$$

In Equation (12), a_1, b_1, c_1, a_2, b_2, c_2, a_3, and b_3 are a new set of eight independent transformation parameters which are functions of the original nine unknowns.

2.3. Registration of Images

Equation (12) can be interpreted as an expression of the transformation relations between a mosaic space (XY-plane) and an image space (xy-plane) without considering non-linear elements and it attempts to get the relationship among several images. In this particular implementation, there is an underlying assumption that the pair of images is related through some sort of planar transformations. Therefore, a spatial relationship between images can be computed based on each pair of images by first, selecting an arbitrary image as a reference image (in the XY system). Once selected, a planar relationship between other images with this reference image is established. Rearranging the Equation (12) such that:

$$\begin{aligned} x + v_x &= a_1X + b_1Y + c_1 - a_3xX - b_3xY \\ y + v_y &= a_2X + b_2Y + c_2 - a_3yX - b_3yY \end{aligned} \quad (14)$$

To facilitate Equation (14) to be used with least squares, the measured x and y coordinates only are considered in the left hand side. The measured values of x, y, X and Y on the right hand side are treated as constants, and then satisfactory results will generally be obtained:

$$\begin{bmatrix} x \\ y \end{bmatrix}_{ij} + \begin{bmatrix} v_x \\ v_y \end{bmatrix}_{ij} = \begin{bmatrix} X & Y & 1 & 0 & 0 & 0 & -xX & -xY \\ 0 & 0 & 0 & X & Y & 1 & -yX & -yY \end{bmatrix}_{ij} \begin{bmatrix} a_1 \\ b_1 \\ c_1 \\ a_2 \\ b_2 \\ c_2 \\ a_3 \\ b_3 \end{bmatrix} \text{ or } {}_{2n}\mathbf{L}_1 + {}_{2n}\mathbf{V}_1 = {}_{2n}\mathbf{A}_{8\,8}\,\mathbf{X}_1 \quad (15)$$

Equations (15) is written for each point pair of the i^{th} pair and the j^{th} point, and since there are eight unknown parameters, the number of n common points or a minimum of four pairs of common points are needed for a unique solution. It strongly recommended that more than four common points be used in the least squares is desirable. Given two images, the target images and the reference image, the goal of the registration problem is to find the vector **X** that transforms the input image into another image similar to the reference or mosaic image. Considering the structure of matrix **A**, the vector **X** is uniquely solved when the numbers of conjugate points are equal to or greater than 4. However, Equation (15) is easily expanded to cope with the number of corresponding points which are greater than four by using the pseudo inverse:

$$\mathbf{X} = \left(\mathbf{A}^{\mathrm{T}}\mathbf{A}\right)^{-1}\mathbf{A}^{\mathrm{T}}\mathbf{L} \quad (16)$$

2.4. Resizable Bounding Box

To figure out the size of the output image we need to compute the maximum extent of each image after it is warped. But we need to specify a reference mosaic at first. This is the image to whose viewpoint all other images will be warped. Because the perspective transformation transforms rectangles into quadrilaterals, all we need to do is to keep track of the four corners of each image to be warped. After warping, we find the minimum and maximum corner coordinates from all the warped corners, and these will determine the bounding box (the smallest rectangle that contains the mosaic). If the corners have coordinates: (1, 1), (cols, 1), (1, rows), and (cols, rows), where cols is the width of each image, and rows is its height. Then, find the minimum and maximum coordinates of the warped corners. These will become the upper left corner and lower right corner of the bounding box respectively. Let (x_{min}, y_{min}); (x_{max}, y_{max}) be these coordinates. Then the width and height of the bounding box are:

$$\text{bWidth} = x_{max} - x_{min} \quad ; \quad \text{bHeight} = y_{max} - y_{min} \quad (17)$$

The computation of the bounding box coordinates is necessary to assist a resampling process which assigns intensity color of each pixel in the mosaic based on the input image's intensity color. These values must be updated after each time the registration process was done.

3. RESULTS AND ANALYSIS

The whole process to produce a single mosaic from any numbers of overlapping images can be summarized as follows:

1. Select the first image as a reference image.
2. Select the next image, compute its perspective transformation parameters
3. Use Bilinear interpolation to assign the color of the new mosaic
4. Repeat step 2-3 for the rest of the images, if overlaps are found, an averaged color can be calculated for the new pixel grid of the mosaic.

The process starts by selecting a supposedly be a vertical reference image and lets set it as the first mosaic. If necessary, this image can be rectified to become a truly vertical image [17] by using its exterior orientation parameters [18]. Next, select an adjacent overlapped image and choose a minimum of four conjugate features appearing on both images. It starts by clicking a feature on the mosaic first to set it as a reference image. On the target image, a location of the conjugate point of the selected feature can be calculated by using the

normalized cross correlation method of Equation (1) to determine an approximate location of the conjugate point. To produce as precise the location of the conjugate point as possible the least squares matching of Equation (10) must be performed to obtain a sub pixel accuracy of the conjugate point.

After a minimum of four conjugate points are selected, a perspective transformation parameter is computed using Equation (16) as well as a new bounding box coordinates of the new mosaic. These parameters are used to resample grid tessellation of the new mosaic with an intensity color. In this research, it has been revealed that bi-linear interpolation is the best choice among the existing techniques available, such as the nearest neighbor, bicubic, and distance weighted average interpolation methods. Among of the first three techniques, the simplest and fastest resampling method in terms of computation time is nearest-neighbor interpolation, which uses the value of the pixel closest to the transformed coordinates. However, since a continuous interpolation is not being performed, the resulting appearance can be very susceptible to aliasing.

Bilinear interpolation, on the other hand, is slower than the nearest neighbor method, and has a smoother appearance effect due to partial elimination of high frequency detail. The bicubic technique is the slowest of the three with regard to computation time, but it is the most rigorous resampling method, and it achieves a smooth appearance without sacrificing too much high frequency detail. Therefore, the bilinear interpolation is preferred over the distance weighted average method since the first gives better results. The experimental result of mosaic from input images is illustrated in Figure 3. It has been shown that seams on the mosaic are spotted due to the fact that we have not implemented color blending or bundle adjustment for global image registration. During experimental testing, it was shown that a local and sequential image registration was performed using Equation (16). This results a significant geometric error budget at the last image registration. An accumulative geometric distortion occurs here as depicted in Figure 3. To remedy this situation it is strongly recommended that simultaneous image registration is used instead.

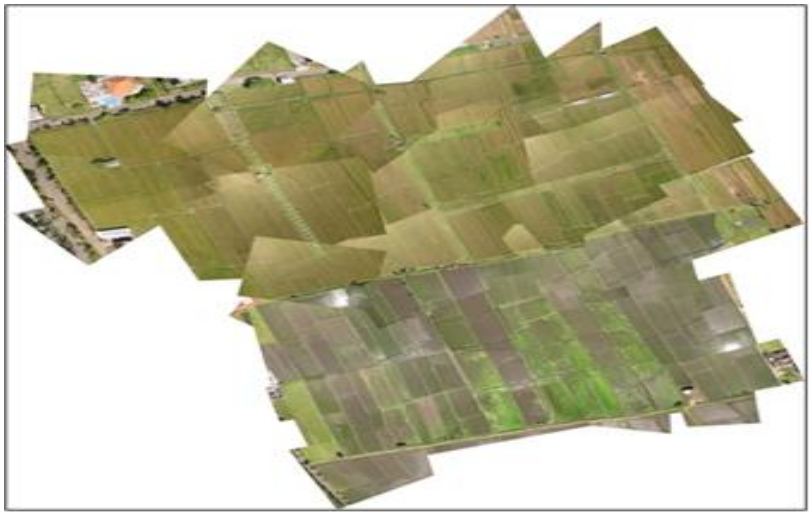

Figure 3. A Mosaic of 36 images with its bounding box: no color blending or lens distortion correction is applied

In contrast with this research finding, Gomez [9] and Tournadre [19] utilize a number of observed GCPs distributed across a surveyed area to improve geometric accuracy of image registration. Then each photo is registered in a sequential order to obtain its exterior orientation parameters using a method described in Tjahjadi [18]. However, the minimum numbers of required GCPs and the spatial distribution of GCPs throughout the survey area are still uncertain. Another method uses a so called Structure From Motion (SfM) to generate a very dense three dimensional point cloud, and these points are incorporated to register images [8, 20-23]. Noticeable drawbacks of the method are that it is very demanding for computer's resources and it is a lack of a consisten validation methodology of image registration quality [20].

On the other hand, our modified collinearity equation generates planar, rectified and ratioed mosaic plane by using a minimum of only four conjugate points from oblique or vertical aerial images. A benefit of our method is the mosaic plane can be made parallel to the datum plane; therefore the resulting mosaic can fit seamlessly with our existed large scale urban city maps. Moreover, the inclusion of GCPs can be readily made in this interactive process to produce an equal scale of rectified aerial images; hence they can be

stitched together on the mosaic plane at an equal image scale. This is usefull for quantitative measurements on the mosaic in our research.

4. CONCLUSION

To sum up, the most important achievement of this paper is a development of a novel mosaicking system which enabling an interactive and a semi automated generation of mosaic based on collinearity condition. This approach combines a classical photogrammetric method as well as computer vision algorithm to generate mosaic. Experimental results show that the method proposed in this paper is effective and feasible for UAV's aerial images. With the proposed methods, a registration of UAV's images could be achieved with low cost and it has a great potential in surveying and urban city mapping. This knowledge and technology will be valuable for native to improve the urban city mapping system, since knowledge is a main factor in the implementation of new technologies [23]. In this preliminary work, no sophisticated color blending is used nor is self-calibrating bundle adjustment performed. As a consequence, the output mosaic may exhibit seams and geometrically incorrect features' appearances. However, a developed C++ program during this research is successfully implemented.

A further improvement to the geometric and radiometric accuracy of the mosaic could be achieved by applying an integration of flight data, GCPs, and other measurements into a rigorous photogrammetric bundle adjustment to make full use of flight data, and by applying feature extraction to make a seamless mosaic. Improving the extraction and matching algorithm combined with other features as well as integrating bundle adjustment into the registration process will be a focus of future research.

ACKNOWLEDGEMENTS

The author wishes to express his sincere thanks to Ministry of Research, Technology and Higher Education of the Republic of Indonesia for supporting a research grant "Hibah Unggulan Perguruan Tinggi", with an announcement letter number 025/E3/2017 and a contract number 073/SP2H/K2/KM/2017.

REFERENCES

[1] Wolf PR, Dewitt BA. *Elements of Photogrammetry: with Applications in GIS, 3rd ed*. New York. McGraw-Hill Companies Inc. 2000: 187-232.
[2] Divya G, Sekhar CC. Image Mosaicing for Wide Angle Panorama. *International Journal of Electrical and Computer Engineering (IJECE)*. 2015; 5(5): 1216-1226.
[3] Joshi H, Sinha K.. A survey on image mosaicing techniques. *International Journal of Advanced Research in Computer Engineering & Technology (IJARCET)*. 2013; 2(2): 365-369.
[4] Bo C, Zhigui L, Junbo W, Yuyu Z. A New Stable and Accurate Algorithm of Large Image Mosaic. *International Journal of Signal Processing, Image Processing & Pattern Recognition*. 2015; 8(6): 215-226.
[5] Pengjun L, Jianzeng L. A Method for UAV's Images seamless Stitching. *Applied Mechanics & Materials.* 2014; 556(562): 5076-5080.
[6] Yan G, Hong X, Lei Y. Research and Analysis of Key Technologies in Image Mosaic. *International Journal of Signal Processing, Image Processing & Pattern Recognition*. 2013; 6(5): 237-244.
[7] Rajithkumar BK. Mohana HS. Template Matching Method for Recognition of Stone Inscripted Kannada Characters of Different Time Frames Based on Correlation Analysis. *International Journal of Electrical and Computer Engineering (IJECE)*. 2014; 4(5): 719-729.
[8] Nex F, Remondino F. UAV for 3D Mapping Applications: a Review. *Applied Geomatics*. 2014; 6(1): 1-15.
[9] Gómez-Candón D, De Castro A, López-Granados F. Assessing the accuracy of mosaics from unmanned aerial vehicle (UAV) imagery for precision agriculture purposes in wheat. *Precision Agriculture*. 2014; 15(1): 44-56.
[10] Gruen AW. Adaptive Least Squares Correlation: A Powerful Image Matching Technique. *South African Journal of Photogrammetry, Remote Sensing and Cartography*. 1985; 14(3): 175-187.
[11] Lemmens MJPM. A Survey on Stereo Matching Techniques. *International Archives of Photogrammetry and Remote Sensing*. 1988; 27(B8): 11-23.
[12] Sahoo SK, Choudhury BB. A Robotic Assistance Machine Vision Technique for An Effective Inspection and Analysis. *International Journal of Electrical and Computer Engineering (IJECE)*. 2015; 5(1): 46-54.
[13] Hamzah RA, Ibrahim H.. Literature Survey on Stereo Vision Disparity Map Algorithms. *Journal of Sensor*. 2016; 1-23.
[14] Mayer H, Sester M, Vosselman G. Basic Computer Vision Technique. *Manual of Photogrammetry 6th Ed. (ASPRS)*. 2013; 517-583.
[15] Calderon F, Romero L. *An Accurate Image Registration Method Using a Projective Transformation Model*. 8th Mexican International Conference on Current Trends in Computer Science ENC. 2007; 58-64.
[16] Kobayashi K, Mori C. Relations between the Coefficients in the Projective Transformation Equations and the Orientation Elements of a Photograph. *Photogrammetric Engineering & Remote Sensing*. 1997; 63(9): 1121-1127.

[17] Novak K. Rectification of Digital Imagery. *Photogrammetric Engineering & Remote Sensing*. 1992; 58(3): 339-344.
[18] Tjahjadi ME. A Fast And Stable Orientation Solution of Three Cameras-Based UAV Imageries. *ARPN Journal of Engineering and Applied Sciences*. 2016; 11(5): 3449-3455.
[19] Tournadre V, Pierrot-Deseilligny M, Faure PH. *UAV Linear Photogrammetry*. The International Archives of the Photogrammetry, Remote Sensing and Spatial Information Sciences. Gottingen. 2015; 327-333.
[20] Smith MW, Carrivick J, Quincey D. Structure from motion photogrammetry in physical geography. *Progress in Physical Geography*. 2016; 40(2): 247-275.
[21] Ai M, Hu Q, Li J, Wang M, Yuan H, Wang S. A robust photogrammetric processing method of low-altitude UAV images. *Remote Sensing*. 2015; 7(3): 2302-2333.
[22] Tonkin TN, Midgley NG, Graham DJ, Labadz JC. The potential of small unmanned aircraft systems and structure-from-motion for topographic surveys: A test of emerging integrated approaches at Cwm Idwal, North Wales. Geomorphology. 2014; 226: 35-43.
[23] Handoko F, Nursanti E, Harmanto D, Sutriono. The Role of Tacit and Codified Knowledge Within Technology Transfer Program on Technology Adaptation. *ARPN Journal of Engineering and Applied Sciences*. 2016; 11(8): 5275-5282.

BIOGRAPHIES OF AUTHORS

Martinus Edwin Tjahjadi obtained his PhD degree in Photogrammetry from the University of Melbourne in 2008. He is currently a Lecturer in Department of Geodesy, Institut Teknologi Nasional (National Institute of Technology (ITN)) Malang, Indonesia. His researh of interest includes photogrammetry, computer vision, and 3D modelling and visualization.

Fourry Handoko is a Lecturer in Industrial Engineering, Institut Teknologi Nasional (National Institute of Technology (ITN)) Malang, Indonesia. He has his PhD for his study in Mechanical and Manufacturing Engineering, the University of Melbourne. Currently, he is also the Chairman of Research and Community Outreach Institution (LPPM) of ITN Malang, Indonesia.

Silvester Sari Sai received the bachelor degree in geodesy engineering from Institut Teknologi Nasional (ITN) Malang, ,Indonesia,in 1996, the master degree in geodesy and geomatics engineering from Institut Teknologi Bandung, Bandung, Indonesia, in 2005. He is currently a Lecturer at the Department of Geodesy, National Institute of Technology (ITN) Malang, Indonesia. His main areas of research interest are point positioning and 3D GIS modelling.